Carbon Transport in MAST

J. McCone[1], N. J. Conway[2], M. Von Hellermann[3], A. R. Field[2], L. Garzotti[2], C. A. Michael[2], A. Patel[2], R. Scannell[2], M. Wisse[2]

[1]*University College Cork, Ireland*
[2]*EURATOM/CCFE Fusion Association, Culham Science Centre, Oxon, OX14 3DB, U.K.*
[3]*FOM Institute Rijnhuizen, Association EURATOM-FOM, Nieuwegein, the Netherlands*

Introduction: Impurities in fusion plasmas dilute the fuel and increase radiation losses reducing core fusion power. At the edge where there is little fusion power, radiation spreads heat loads reducing damage to plasma facing materials. Thus measuring the impurity distribution, as well as overall concentration is important in order to identify regimes achieving hollow profiles, where impurity concentrations are highest at the plasma edge. Recent analysis of carbon charge exchange emission data was undertaken on MAST and C^{6+} density profiles are now routinely calculated at 1cm spatial resolution. This paper presents a summary of the typical carbon density distributions observed on MAST in various scenarios along with preliminary analysis.

Carbon Densities Measured by Charge eXchange Recombination Spectroscopy (CXRS): CX emission occurs as excited ions created by electron transfer from donor atoms, transit to lower energy states. Emission brightness varies with the product of neutral donor atom and acceptor ion density in the plasma. As most carbon CX emission in the plasma centre is a result of charge exchange from the neutral beam, carbon density is given by the expression:

$$n_c = \frac{4\pi B}{\sum_{j=1}^{3} \left\langle \sigma v \right\rangle^{j} \left\langle n_b^{j} \right\rangle L}$$

where n_c is carbon density, B is CX emission brightness, $\langle n_b^j \rangle$ is sight line averaged beam neutral density for each given energy species j, $\langle \sigma v^j \rangle$ is the charge exchange emission rate coefficient and L is sight line length. CX emission is measured on MAST by a high spatial resolution (~1cm) spectrometer CELESTE-3 [1]. The measured beam power and known beam geometry is input into a code to calculate the beam attenuation and from this beam density using stopping coefficients obtained from ADAS[2]. Due to uncertainties in ADAS cross-sections and beam species fractions, errors are hard to estimate so cross diagnostic consistency checks are essential.

Data Consistency Checks: To check the modelled beam density, the beam D_α emission was predicted using the beam density, electron density (n_e) and ADAS D_α rate coefficients. This was compared with measured beam D_α emission. The ratio between measured and predicted

emission varied by only ~15% at different radial points in spite of a factor of 5 difference in beam attenuation between these locations giving confidence in the beam stopping coefficients used. While the ratio was close to constant, it was ~0.7 and not unity. Other tokamaks show similar disagreement between predicted and measured D_α [3]. This discrepancy is now believed to be due to the effect of the motional Stark electric field on the n=3 population [4] altering the neutral beam's D_α rate coefficients. New D_α coefficients have recently been calculated taking this effect into account, however this new data has not yet been used at MAST. Thus beam density was not inferred from beam D_α but was taken from the code.

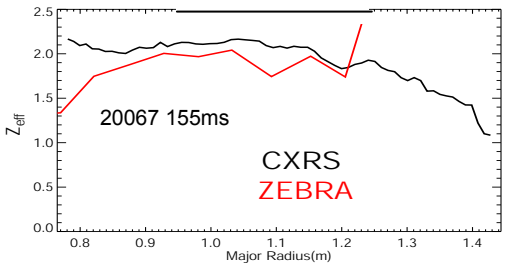

Fig.1 Z_{eff} profiles from CXRS (black) and ZEBRA (red) for L-mode plasmas

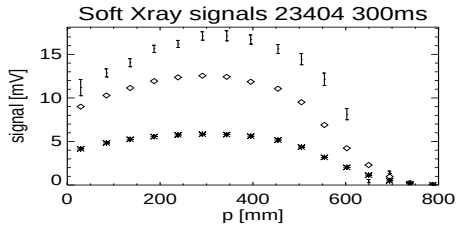

Fig. 2 Forward modelled soft X-rays using Z_{eff}=1 (asterisks), CXRS Z_{eff} (diamonds) and experiment (bars)

Z_{eff} profiles calculated from carbon densities (CXRS) assuming carbon to be the dominant impurity, were compared to visible bremsstrahlung Z_{eff} profiles from the ZEBRA[5] diagnostic (Fig. 1.). The profiles had similar central Z_{eff} in L-mode with disagreement at edge due to molecular emission and partial ionization of carbon while in H-mode Z_{eff} from CXRS and ZEBRA tended to differ in magnitude though the shapes of both profiles looked similar. A comparison with the forward modelled soft X-rays using Z_{eff} from carbon agreed better with the measurement than when Z_{eff} =1 was assumed (Fig. 2.).

Observations: MAST carbon densities typically exhibit 3 main profile categories, (Fig. 3.), centrally peaked profiles both in Z_{eff} and n_c (a), profiles with slight peaking in n_c but with flat Z_{eff} (b) and finally hollow n_c profiles (c). Highly peaked profiles are typical immediately after the start of NBI heating while plasmas are still Ohmic-like. These impurity profiles show similarities to Ohmic profiles observed at CDX-U[6]. In MAST they are typified by a low,

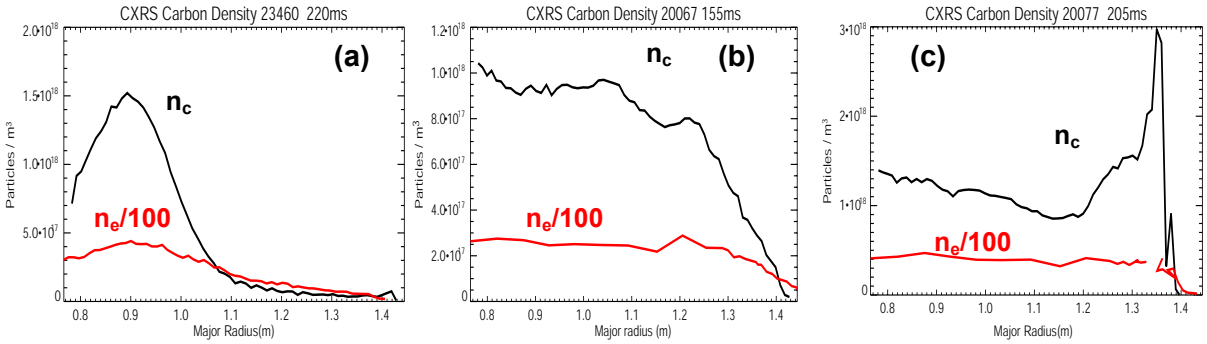

Fig 3. 3 carbon profile types mainly observed at (Left) beam cut on, (centre) L-mode and (right) H-mode

flat level of impurities outside r/a ~0.5 with an increase in the n_c gradient inside (often coinciding with negative shear region) and high central impurity concentrations. This profile type is also seen well after the beam starts in discharges with counter current beam injection and in cases of co-current injection with ITBs. Discharges with high central n_c usually also show central peaking for n_e, though this is less pronounced. Weak centrally peaked profiles with flat Z_{eff} profiles are typical of L-modes without ITBs. Hollow impurity profiles are typical of H- modes. Both L-modes and H-modes occasionally have carbon density "bumps" localized at mid-radius which are also sometimes observed in n_e by Thomson Scattering (Fig. 4). Preliminary investigation of these bumps show they have a tendency to occur in regions of minimum absolute shear close to the q=1 surface during weak ITBs. Similar mid-radius bumps have been observed on JET[7] and NSTX[8]. In addition to generic profile features, transient events (Fig. 5) also can have a large impact on carbon profiles. Large amounts of carbon were seen to migrate towards the plasma centre from the edge following an Internal Reconnection Event (IRE) that occurred during H-mode. Inwards migration of carbon was also observed following pellet injection. Finally a fast rotating snake picked up on the soft X-rays caused a 90% reduction in core n_c. If future reactors are to have finely tuned impurity profiles, sensitivity to these kind of events must be noted.

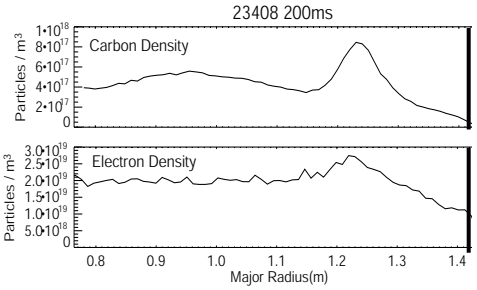

Fig. 4 mid-radius bump in carbon (top) from CXRS radially coincides with bump in electron density seen by Thomson Scattering (bottom)

Neoclassical Carbon Transport Comparisons: The module NCLASS[9] was run through the driver code FORCEBAL for sample MAST pulses to calculate neoclassical predictions for the diffusion coefficient and convection velocity, while the experimental diffusion to convection ratios for carbon impurities were obtained from the carbon profile shape using the article flux equation:

$$\Gamma_c = -D\frac{\partial n_c}{\partial r} + vn_c$$

Where Γ_c is the carbon flux, D is the impurity diffusion coefficient and v is the impurity convection velocity. In steady state ($\Gamma_c = 0$), the inverse scale length of carbon ($1/L_c = \partial n_c/\partial r \,/\, n_c$), is

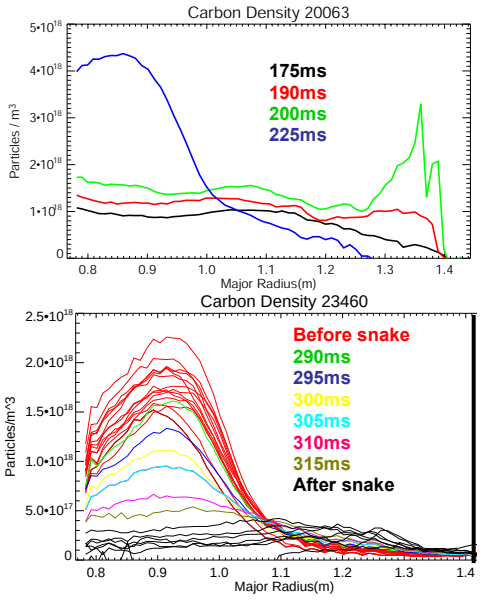

Fig. 5 Effect of IRE at 210ms for shot 20063 (top) and snake at 290ms for shot 23460 (bottom)

equal to the ratio (v/D). Agreement indicates that neoclassical effects dominate impurity transport while disagreement indicates anomalous effects dominate. FORCEBAL was run for time slices where carbon densities remained steady for >15ms and the output v/D ratios were compared to $1/L_c$ (Fig. 6). In many cases, the (v/D) terms' magnitudes were similar in size to $1/L_c$, but had opposite sign. When inverted the v/D profile shared many qualitative short scale length radial features with $1/L_c$. This is being investigated further.

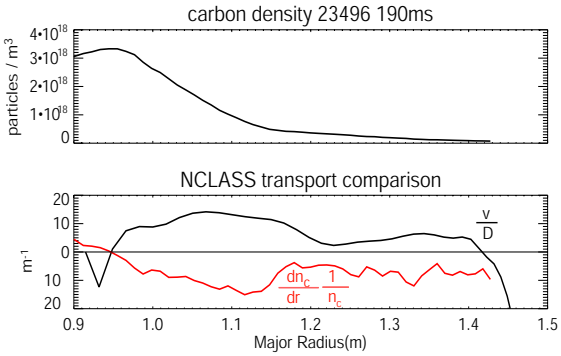

Fig. 6 v/D ratio calculated by FORCEBAL for L-mode pulse compared with inverse impurity scale length (bottom) for carbon density profile (top)

Summary

MAST H-modes frequently displayed hollow impurity profiles that in principle would be beneficial for a reactor, however whether these can be maintained in steady state for long periods remains uncertain. Many observations of MAST carbon behaviour, such as mid-radius peaking are similar to observations on other machines[7][8]. Central accumulation was observed to occur slowly during ITBs and rapidly after Internal Reconnection Events while snake-like instabilities were seen to flush impurities from the core without significant temperature reduction. These marked differences demonstrate that MAST carbon profiles are highly sensitive to plasma conditions so understanding the effect of plasma events on impurity distribution is essential for the impurity seeded plasmas of future reactors. Preliminary comparisons of carbon density gradients with neoclassical v/D ratios from FORCEBAL have been made though further investigation will be required to form definite conclusions.

[1] N. J. Conway et al., Review of Scientific Instruments **77**(10) Oct. 2006 p10F131-(1-3)

[2] ADAS website: www.adas.ac.uk

[3] http://www.lorentzcenter.nl/lc/web/2009/348/presentations/Delabie.pdf E. Delabie e.delabie@fz-juelich.de

[4] O Marchuk, Jounal of Physics B : Atomic and Molecular Optic Physics **43** (2010) 011002 (6pp)

[5] A. Patel et al, Review of Scientific Intruments **75**(11) Nov 2004 p 4944-4950

[6] V. A. Soukhanovskii et al, Plasma Physics and Controlled Nuclear Fusion **44** (2002) p2339-2355

[7] H. Chen et al, Nuclear Fusion **41**(1) 2001 p31-46

[8] D. Stutman et al, Physics of Plasmas **10**(11) Nov 2003 p4387-4395

[9] W. A. Houlberg et al., Physics of Plasmas **4**(9) Sept 1997 p3230-3242

This work was funded by the Engineering and Physical Sciences Research Council under grant EP/G003955 and the European Communities under the contract of Association between EURATOM and CCFE. The views and opinions expressed herein do not necessarily reflect those of the European Commission.Thanks to Wayne Houlberg for explaining the details of FORCEBAL.